Nigerian Research Journal of Engineering and Environmental Sciences 3(1) 2018 pp. 125-139

Nigerian Research Journal of Engineering and Environmental Sciences
Journal homepage: www.rjees.com

Original Research Article

ANALYSIS OF A FLUID-CONTAINING SHELL OF SEGMENTED TOROIDAL FORM

[1]Enoma, N. and *[2]Igbinomwanhia, N.

[1]Structural Engineering & Mechanics Research Group, University of Cape Town, South Africa.
[2]Department of Mechanical Engineering, Faculty of Engineering, University of Benin, Benin City, Nigeria.
*noel.igbinomwanhia@uniben.edu

ARTICLE INFORMATION

Article history:
Received 02 March, 2018
Revised 05 May, 2018
Accepted 07 May, 2018
Available online 30 June, 2018

Keywords:
Containment vessel
Membrane hypothesis
Multi-shell toroid
Shell analysis
Toroidal tank

ABSTRACT

A novel toroidal shell form for liquid containment is proposed in this paper. The vessel comprises four smoothly joined toroidal segments, and the linear elastic theory of shells of revolution is adopted in the formulation of closed-form membrane solutions for the toroid. The presented algorithm for the evaluation of membrane stresses and deformations in liquid-filled segmented toroidal tanks is demonstrated through a numerical example. Some useful insight and a set of design recommendations are provided. The obtained analytical results can also be employed in the determination of bending disturbances at the junctions of the vessel, and for other specialized studies on shells of this type.

1. INTRODUCTION

Containment shell structures are widely used throughout the world for holding water in the form of elevated tanks, and for the storage of petroleum products, chemicals and liquefied gases. The commonest class of shell structures for these applications are shells of revolution. Typical examples are cylindrical, spherical, conical and ellipsoidal tanks. Cylindrical tanks being the convectional liquid-containment vessels have received a considerable amount of attention in the literature (Guggenberger, 1994; Rotter, 1998; Sosa et al., 2006; Taniguchi, Ando and Nakashima, 2009; Ozdemir, Souli and Fahjan, 2010; Sosa and Godoy, 2010; Burgos *et al.*, 2014). Toroidal shells are not a very common type of shells of revolution. A couple of studies have been conducted to understand the behaviour of these shell forms (Zhang *et al.*, 1998; Redekop, Xu and Zhang, 1999; Kuznetsov and Levyakov, 2001; Teng, Yuan and Wang, 2002; Velickovic, 2007; Zhan and Redekop, 2008; Zu *et al.*, 2012a, 2012b). Owing to the structural efficiency of shells of double curvatures and the advantages of combining shells with basic mathematical profiles to form compound shells, it is almost possible to obtain a desired structural shell form for liquid containment. Some recently proposed compound vessels may be found in (Zingoni, 2001a, 2001b, 2002, 2004; Zingoni et al., 2015). The present study involves the static analysis of liquid-filled multi-segmented toroids, first reported in (Enoma and Zingoni, 2016, Enoma and Zingoni, 2017) for a uniform pressure loading condition. Based on the linear

elastic theory of shells of revolution, explicit expressions are derived here for the determination of membrane stresses and deformations that occur within the segmented toroids under hydrostatic pressure loading which, of course, varies across the height of the vessel. A numerical example is conducted on a toroid that is asymmetrical about the equatorial plane. The vessel is assumed to be completely-filled with water of approximate specific weight $\gamma = 10 \times 10^3 \ N/m^3$

2. GEOMETRY

The liquid-filled toroidal shell of multi-segmented spherical cross-section under consideration comprises an upper toroidal segment with a local cross-sectional circular segment of radius a_1 (centre C_1) and a lower toroidal segment with a local cross-sectional circular segment of radius a_1 (centre C_3), these are connected tangentially by two middle toroidal segments - one in the outer region and the other in the inner region of the toroid; with local cross sectional circular segments of radii a_2^o (centre C_2^o) and a_2^i (centre C_2^i) respectively. To reduce complexity, a_2^i and C_2^i are not shown in Figure 1. The junctions D_1^o, D_2^o, D_1^i, and D_2^i of the four toroidal segments of the vessel exhibit no slope discontinuity, but an abrupt jump in the local radius from one segment to the other.

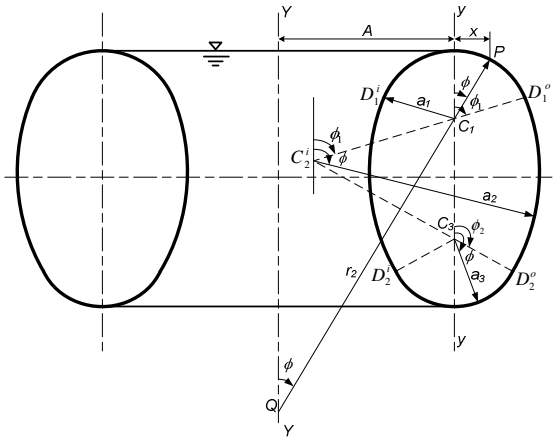

Figure 1: Geometric parameters of the liquid-filled toroidal tank

In Figure 1, A is the mean toroidal radius (the distance between the vertical axis of revolution Y-Y of the segmented toroid and the local centreline y-y) and ϕ is the angular coordinate measuring the angle from the upward direction of the axis of revolution of the shell to the normal to the shell middle surface at any point P in question. With this definition of ϕ, two points - one in the outer region and the other in the inner region of the toroid are located for one value of ϕ. To distinguish between these two points, when viewing the cross-sectional profile to the right of the vertical axis of revolution Y-Y, we may consider all shells to the right side of the local toroidal centreline y-y to be in the outer region of the toroid, while the shells to the left side of the local toroidal centreline y-y to be in the inter-region of the toroid. Consequently, the segmented toroidal vessel consists of six regions: the upper-outer, middle-outer, lower-outer, lower-inner, middle-inner, and upper-inner regions. The values of ϕ at junctions D_1^o, D_2^o, D_1^i, and D_2^i are ϕ_1^o, ϕ_2^o, ϕ_1^i, and ϕ_2^i, respectively, as shown. In the present study, focus is on the stresses and deformations that occur throughout

the shell, but the precise support location and conditions of the shell in the immediate vicinity of support lines will not be pursued.

x is the horizontal coordinate measuring the distance between the local centreline y-y and any point *P* in the middle surface of the shell. That is:

$$x_1 = \pm a_1 \sin\phi \tag{1a}$$

for the upper regions:

$$x_2 = \pm\left(a_2 \sin\phi - q\right) \tag{1b}$$

for the middle regions, and

$$x_3 = \pm a_3 \sin\phi \tag{1c}$$

for the lower regions:

where for the sign ($\pm$), the plus sign applies to points in the outer region, while the minus sign applies to points in the inner regions of the toroid; $a_2 = a_2^o = a_2^i$; $\sin\phi_1 = \sin\phi_1^o = \sin\phi_1^i$; $\sin\phi_2 = \sin\phi_2^o = \sin\phi_2^i$ and $q = \left(a_2 - a_1\right)\sin\phi_1$.

A point in the middle surface of the segmented toroidal shell may be characterized by r_1 and r_2 (the principal radii of curvature of the shell middle surface in the meridional plane and the second principal plane respectively). The first principal radius of curvature of the toroidal surface at any point P is the actual radius of curvature r_1 of the local profile at that point, while the second principal radius of curvature r_1 is equal to the distance *PQ*, where *Q* is the point at which the surface normal at *P* intersect the axis of revolution Y-Y of the toroid. These may be expressed as:

$$r_1 = a \tag{2}$$

note that r_1 for the inner region of the toroid being on the side of the shell surface opposite to that on which the axis of revolution lies, must be taken as negative, and

$$r_2 = \frac{A + x}{\sin\phi} \tag{3}$$

where *a* is the local radius of a particular segment under consideration and *x* is as respectively defined in Equations 1.

3. LOADING PRELIMINARIES

Assuming the toroidal shell with multi-segmented spherical cross-section is internally filled with liquids of specific weight γ. For the axisymmetrically loaded vessel, the loading components p_ϕ and p_θ (per unit area of shell middle surface) in the meridional and hoop directions, respectively, are each equal to zero, since hydrostatic pressure acts purely perpendicular to the shell middle surface. The loading component P_r (per unit area of shell middle surface) due to the internal pressure loading from the contained liquid, acting normal to the shell middle surface is considered positive if pointing away from the axis of revolution of the shell (i.e outer region of the vessel), while negative if pointing towards the axis of revolution of the shell (i.e inner region of the vessel), may be expressed as:

$$P_r = \pm \gamma h \tag{4}$$

where *h* is:

$$h_1 = a_1(1 \mp \cos\phi) \tag{5a}$$

for the upper regions:

$$h_2 = h_{D_1} \pm a_2(\cos\phi_1 - \cos\phi) \tag{5b}$$

for the middle regions:

$$h_3 = h_{D_2} \pm a_3(\cos\phi_2 - \cos\phi) \tag{5c}$$

for the lower regions:

and for the double operations, the upper sign applies to the outer region, while the lower sign applies to the inner regions of the toroid, $h_{D_1} = a_1(1 \mp \cos\phi_1)$, $h_{D_2} = h_{D_1} + a_2(\cos\phi_1 - \cos\phi_2)$.

4. MEMBRANE SOLUTION

An elemental shell of revolution in equilibrium under axisymmetric loading conditions is shown in Figure 2. The general expressions for the membrane stress resultants and deformations as given in (Flügge, 1973; Zingoni, 1997) are, taking $p_\phi = 0$:

$$N_\phi^m = \frac{1}{r_2 \sin^2\phi}\left[\int r_1 r_2 p_r \cos\phi \sin\phi d\phi\right] \tag{6}$$

$$N_\theta^m = r_2\left(p_r - \frac{N_\phi^m}{r_1}\right) \tag{7}$$

$$\delta^m = \frac{1}{Et}(r_2 \sin\phi)\left(N_\theta^m - \nu N_\phi^m\right) \tag{8}$$

$$V^m = \frac{1}{r_1}\left[\frac{\cot\phi}{Et}\left\{(r_1 + \nu r_2)N_\phi^m - (r_2 + \nu r_1)N_\theta^m\right\} - \frac{d}{d\phi}\left\{\frac{r_2}{Et}\left(N_\theta^m - \nu N_\phi^m\right)\right\}\right] \tag{9}$$

In these expressions, N_ϕ^m and N_θ^m are the membrane stress resultants in the meridional and hoop directions respectively; these are forces per unit length of the respective edge of the shell element, considered positive when tensile, δ^m is the horizontal displacement of a point on the shell meridian, considered positive when away from the axis of revolution, V^m is the rotation of the tangent to the shell meridian at any point on the shell, considered positive when the tangent rotates clockwise on the side of the shell cross-section to the right of the axis of revolution, *E* is the young's modulus of elasticity of the shell material, *v* is its Poisson's ratio, *t* is the shell thickness and all other terms are as previously defined.

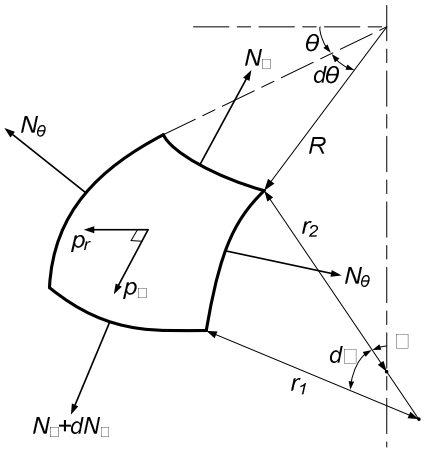

Figure 2: Element of the axisymmetrically loaded shell of revolution

4.1. Outer Region of the Tank

For the upper-outer region of the tank, using Equations (2) - (4) to eliminate r_1, r_2 and p_r in Equation (6), and evaluating the integral, we obtain after some simplifications, the meridional stress resultant:

$$\left(N_{\phi}^{m}\right)_1^o = \frac{\gamma a_1^2}{6\sin\phi\left(A + a_1\sin\phi\right)}\left\{a_1\left(-3+2\cos\phi\right)\cos^2\phi \;\; -3A\left(\phi+\left(-2+\cos\phi\right)\sin\phi\right)+C_1^o\right\} \tag{10}$$

where C_1^o is the constant of integration to be determined from a suitable boundary condition. At $\phi = 0$, $\left(N_{\phi}^{m}\right)_1^o$ must be zero. This condition gives $C_1^o = a_1$, so that:

$$\left(N_{\phi}^{m}\right)_1^o = \frac{\gamma a_1^2}{6\sin\phi\left(A + a_1\sin\phi\right)}\left\{a_1\left(1+\left(-3+2\cos\phi\right)\cos^2\phi\right) - 3A\left(\phi+\left(-2+\cos\phi\right)\sin\phi\right)\right\} \tag{11}$$

With $\left(N_{\phi}^{m}\right)_1^o$ now known, the membrane stress resultant in the hoop direction follows from expression (7) which after eliminating r_1, r_2 and p_r for the upper-outer region of the vessel, may be written as:

$$\left(N_{\theta}^{m}\right)_1^o = \frac{\gamma a_1}{6\sin^2\phi}\left\{4a_1\left(5+4\cos\phi\right)\sin^4\left(\frac{\phi}{2}\right)+3A\left(\phi-\cos\phi\sin\phi\right)\right\} \tag{12}$$

Substituting Equations (2), (3), (4), (11) and (12) for the upper-outer region of the toroidal tank into Equations (8) and (9), we obtain after some simplifications, the deformations:

$$\left(\delta^m\right)_1^o = \frac{\gamma a_1}{6Et\sin\phi}\left[\frac{\left(A+a_1\sin\phi\right)}{\sin\phi}\left\{4a_1\left(5+4\cos\phi\right)\sin^4\left(\frac{\phi}{2}\right)+3A\left(\phi-\cos\phi\sin\phi\right)\right\}\right.$$
$$\left.-a_1\nu\left\{a_1\left(1+\left(-3+2\cos\phi\right)\cos^2\phi\right)-3A\left(\phi+\left(-2+\cos\phi\right)\sin\phi\right)\right\}\right] \tag{13}$$

and

$$\left(V^m\right)_1^o = -\frac{\gamma}{48Et\sin^4\phi\left(A+a_1\sin\phi\right)}\left\{48a_1^3\sin^6\phi+96a_1^2A\sin^5\left(\frac{\phi}{2}\right)\left(25\cos\left(\frac{\phi}{2}\right)\right.\right.$$
$$\left.\left.+11\cos\left(\frac{3\phi}{2}\right)+2\cos\left(\frac{5\phi}{2}\right)\right)+a_1A^2\left(81-32\cos\phi-56\cos2\phi+7\cos4\phi\right.\right.$$

$$-36\phi\sin 2\phi)+48A^3(-\phi\cos\phi+\sin\phi)\} \tag{14}$$

For the middle-outer region of the vessel, substituting Equations (2), (3), and (4) into Equation (6), we obtain after some simplifications, the meridional stress resultant

$$\left(N_\phi^m\right)_2^o=\frac{\gamma}{12(A-q\ +a_2\sin\phi)\sin\phi}\left[a_2\{a_2^2(3\cos\phi\ +\cos3\phi-3\cos\phi_1\cos2\phi)-3a_2((A-q)\right.$$
$$\left.(2\phi-4\cos\phi_1\sin\phi+\sin2\phi)+h_{D_1}cos2\phi)+12h_{D_1}(A-q)\sin\phi\}+C_1^o\right] \tag{15}$$

C_1^o is obtained from the condition that N_ϕ^m in the upper-outer region of the vessel and in the middle-outer region of the vessel must have the same values at the junction $\phi=\phi_1$ of the two regions. This condition gives

$$C_1^o=8a_1^3(1+2\cos\phi_1)Sin^4\left(\frac{\phi_1}{2}\right)-3a_1a_2\sin\phi_1(4h_{D_1}\sin\phi_1+a_2(\sin2\phi_1-2\phi_1))-3Aa_1^2$$
$$(-4\sin\phi_1+\sin2\phi_1+2\phi_1)-a_2\{12Ah_{D_1}\sin\phi_1+3a_2(h_{D_1}(-2+\cos2\phi_1)+A(\sin2\phi_1$$
$$-2\phi_1))+a_2^2(\cos3\phi_1+6\phi_1\sin\phi_1)\} \tag{16}$$

With $\left(N_\phi^m\right)_2^o$ now known, the membrane stress resultant in the hoop direction follows from expression (7) which after eliminating r_1, r_2 and p_r for the middle-outer region of the tank, may be written as:

$$\left(N_\theta^m\right)_2^o=-\frac{\gamma}{12a_2\sin^2\phi}\left[-a_2^3(-2+\cos2\phi)(4\cos\phi-3\cos\phi_1)+3a_2^2\{(A-q)(-2\phi\right.$$
$$\left.+\sin2\phi)+h_{D_1}(-2+\cos2\phi)\}+C_1^o\right] \tag{17}$$

The deformations follow by substituting Equations (2), (3), (15) and (17) for the middle-outer region of the toroidal vessel into Equations (8) and (9):

$$\left(\delta^m\right)_2^o=\frac{\gamma}{12Et\sin\phi}\left[-\frac{A-q+a_2\sin\phi}{a_2\sin\phi}\{-a_2^3(-2+\cos2\phi)(4\cos\phi-3\cos\phi_1)\right.$$
$$+3a_2^2\{(A-q)(-2\phi+\sin2\phi)+h_{D_1}(-2+\cos2\phi)\}+C_1^o\}$$
$$-\nu\{a_2^3(3\cos\phi\ +\cos3\phi-3\cos\phi_1\cos2\phi)-3a_2^2((A-q)(2\phi-4\cos\phi_1\sin\phi$$
$$\left.+\sin2\phi)+h_{D_1}cos2\phi)+12a_2h_{D_1}(A-q)\sin\phi+C_1^o\}\right] \tag{18}$$

and

$$\left(V^m\right)_2^o=\frac{\gamma}{48Eta_2^2\sin^4\phi(A-q+a_2\sin\phi)}\left[-48a_2^5\sin^6\phi+6a_2^4(A-q)\sin\phi\{-14+8\cos2\phi\right.$$
$$-2\cos4\phi+\cos\phi_1(7\cos\phi-\cos^3\phi+3\cos\phi\sin^2\phi)\}+a_2^3(A-q)\{(A-q)(-81$$
$$+56\cos2\phi-7\cos4\phi+24\cos\phi_1\cos\phi+36\phi\sin2\phi)-3h_{D_1}(-8\sin2\phi+\sin4\phi)\}$$
$$+24a_2^2(A-q)^2\{2(A-q)(\phi\cos\phi-\sin\phi)+h_{D_1}\cos\phi\}-2(A-q)C_1^o\{4(A-q)$$
$$\left.\cos\phi+3a_2sin2\phi\}\right] \tag{19}$$

For the lower-outer region of the tank, substituting Equations (2), (3), and (4) into Equation (6) and evaluating the integral, and using the condition that N_{ϕ}^{m} in the middle-outer region of the vessel and in the lower-outer region of the vessel must have the same values at the junction $\phi=\phi_2$ of the two regions, we obtain after some simplifications, the meridional stress resultant:

$$\left(N_{\phi}^{m}\right)_3^o = \frac{\gamma}{12\sin\phi\left(A+a_3\sin\phi\right)}\left\{2a_3^3\cos^2\phi\left(2\cos\phi-3\cos\phi_2\right)-3a_3^2\left(A(2\phi-4\cos\phi_2\sin\phi+\sin 2\phi)+2h_{D_2}\cos^2\phi\right)+12a_3Ah_{D_2}\sin\phi+C_2^o\right\} \tag{20}$$

Where:

$$\begin{aligned} C_2^o = -a_3\Big\{&-2a_3^2\cos^3\phi_2+12Ah_{D_2}\sin\phi_2+3a_3\left(-2h_{D_2}\cos^2\phi_2+A(\sin 2\phi_2-2\phi_2)\right)\Big\} \\ &+\frac{A+a_3\sin\phi_2}{A+a_2\sin\phi_2+(a_1-a_2)\sin\phi_1}\Big\{a_2^3\left(3\cos\phi_2-3\cos\phi_1\cos 2\phi_2+\cos 3\phi_2\right) \\ &-3a_2^2\left(h_{D_1}\cos 2\phi_2+(A+(a_1-a_2)\sin\phi_1)(-4\cos\phi_1\sin\phi_2+\sin 2\phi_2+2\phi_2)\right) \\ &+12a_2h_{D_1}\sin\phi_2\left(A+(a_1-a_2)\sin\phi_1\right)+C_1^o\Big\} \end{aligned} \tag{21}$$

The hoop stress resultant follows as:

$$\left(N_{\theta}^{m}\right)_3^o = -\frac{\gamma}{12a_3\sin^2\phi}\left\{a_3^3\left(6\cos\phi-2\cos 3\phi+3\cos\phi_2(-3+\cos 2\phi)\right)+3a_3^2\left(A(-2\phi+\sin 2\phi)+h_{D_2}(-3+cos2\phi)\right)+C_2^o\right\} \tag{22}$$

Similarly, the deformations are:

$$\begin{aligned} \left(\delta^m\right)_3^o = \frac{\gamma}{12Et\sin\phi}\Bigg[&-\left(\frac{A}{a_3\sin\phi}+1\right)\Big\{a_3^3\left(6\cos\phi-2\cos 3\phi+3\cos\phi_2(-3+\cos 2\phi)\right) \\ &+3a_3^2\left(A(-2\phi+\sin 2\phi)+h_{D_2}(-3+cos2\phi)\right)+C_2^o\Big\}-\nu\Big\{2a_3^3\cos^2\phi\left(2\cos\phi\right. \\ &\left.-3\cos\phi_2\right)-3a_3^2\left(A(2\phi-4\cos\phi_2\sin\phi+\sin 2\phi)+2h_{D_2}\cos^2\phi\right) \\ &+12a_3Ah_{D_2}\sin\phi+C_2^o\Big\}\Bigg] \end{aligned} \tag{23}$$

and

$$\begin{aligned} \left(V^m\right)_3^o = \frac{\gamma}{48Eta_3^2\sin^4\phi\left(A+a_3\sin\phi\right)}\Big[&-48a_3^5\sin^6\phi+6a_3^4A\sin\phi\{-14+8\cos 2\phi \\ &-2\cos 4\phi+\cos\phi_2\left(13\cos\phi-\cos^3\phi+3\cos\phi\sin^2\phi\right)\}+a_3^3A\{A(-81 \\ &+56\cos 2\phi-7\cos 4\phi+48\cos\phi_2\cos\phi+36\phi\sin 2\phi)-3h_{D_2}\left(-14\sin 2\phi\right. \\ &\left.+\sin 4\phi\right)\}+48a_3^2A^2\left\{A\left(\phi\cos\phi-\sin\phi\right)+h_{D_2}\cos\phi\right\} \end{aligned}$$

$$-2AC_2^o\{4A\cos\phi+3a_3 sin2\phi\}] \tag{24}$$

4.2. Inner Region of the Tank

For the upper-inner region of the tank, using appropriate equations (2) - (4) to eliminate r_1, r_2 and p_r in Equation (6), and evaluating the integral, we obtain after some simplifications, the meridional stress resultant:

$$\left(N_\phi^m\right)_1^i=\frac{\gamma a_1^2}{6\sin\phi(A-a_1\sin\phi)}\{a_1(3+2\cos\phi)\cos^2\phi + 3A(\phi+(2+\cos\phi)\sin\phi)+C_1^i\} \tag{25}$$

where C_1^i is the constant of integration to be determined from a suitable boundary condition. At $\phi=\pi$, $\left(N_\phi^m\right)_1^i$ must be zero. This condition gives $C_1^i=-(a_1+3A\pi)$, so that:

$$\left(N_\phi^m\right)_1^i=\frac{\gamma a_1^2}{6\sin\phi(A-a_1\sin\phi)}\{a_1((1+\cos\phi)^2(-1+2\cos\phi)) + 3A(-\pi+\phi+(2+\cos\phi)\sin\phi)\} \tag{26}$$

With $\left(N_\phi^m\right)_1^i$ now known, the membrane stress resultant in the hoop direction follows from Equation (7) which after eliminating r_1, r_2 and p_r for the upper-inner region of the vessel, may be written as:

$$\left(N_\theta^m\right)_1^i=-\frac{\gamma a_1}{6\sin^2\phi}\left\{4a_1(-5+4\cos\phi)\cos^4\left(\frac{\phi}{2}\right)+3A(\pi-\phi+\cos\phi\sin\phi)\right\} \tag{27}$$

Substituting Equations (2), (3), (4), (26) and (27) for the upper-inner region of the toroidal tank into equations (8) and (9) we obtain after some simplifications, the deformations:

$$\left(\delta^m\right)_1^i=\frac{\gamma a_1}{6Et\sin\phi}\left[-\frac{(A-a_1\sin\phi)}{\sin\phi}\left\{4a_1(-5+4\cos\phi)\cos^4\left(\frac{\phi}{2}\right)+3A(\pi+\cos\phi\sin\phi - \phi)\right\}-a_1\nu\{a_1((1+\cos\phi)^2(-1+2\cos\phi))+3A(-\pi+\phi+(2+\cos\phi)\sin\phi)\}\right] \tag{28}$$

and

$$\left(V^m\right)_1^i=\frac{\gamma}{48Et\sin^4\phi(A-a_1\sin\phi)}\left\{-48a_1^3\sin^6\phi+96a_1^2A\cos^5\left(\frac{\phi}{2}\right)\left(25\sin\left(\frac{\phi}{2}\right)-11\sin\left(\frac{3\phi}{2}\right)+2\sin\left(\frac{5\phi}{2}\right)\right)-a_1A^2(81+32\cos\phi-56\cos2\phi+7\cos4\phi + 36(\pi-\phi)\sin2\phi)+48A^3((\pi-\phi)\cos\phi+\sin\phi)\right\} \tag{29}$$

For the middle-inner region of the vessel, substituting Equations (2), (3), and (4) into Equation (6), we obtain after some simplifications, the meridional stress resultant

$$\left(N_\phi^m\right)_2^i=\frac{\gamma}{12(A+q\ -a_2\sin\phi)\sin\phi}\{a_2^3(3\cos\phi+\cos3\phi-3\cos\phi_1\cos2\phi)+3a_2^2((A+q)(2\phi-4\cos\phi_1\sin\phi+\sin2\phi)+h_{D_1}cos2\phi)+12a_2h_{D_1}(A+q)\sin\phi+C_1^i\} \tag{30}$$

C_1^i is obtained from the condition that N_ϕ^m in the upper-inner region of the vessel and in the middle- inner region of the vessel must have the same values at the junction $\phi=\phi_1$ of the two regions. This condition gives

$$C_1^i = 8a_1^3(-1+2\cos\phi_1)\cos^4\left(\frac{\phi_1}{2}\right)+3a_1a_2\sin\phi_1\left(4h_{D_1}\sin\phi_1-a_2(\sin2\phi_1-2\phi_1)\right)+3Aa_1^2$$
$$(-2\pi+4\sin\phi_1+\sin2\phi_1+2\phi_1)-a_2\{12Ah_{D_1}\sin\phi_1-3a_2\left((-2+\cos2\phi_1)h_{D_1}\right.$$
$$\left.+A(\sin2\phi_1-2\phi_1)\right)+a_2^2\left(\cos3\phi_1+6\phi_1\sin\phi_1\right)\} \quad (31)$$

With $\left(N_\phi^m\right)_2^i$ now known, the membrane stress resultant in the hoop direction follows from Equation (7) which after eliminating r_1, r_2 and p_r for the middle-inner region of the tank, may be written as

$$\left(N_\theta^m\right)_2^i = \frac{\gamma}{12a_2\sin^2\phi}\left[-a_2^3(-2+\cos2\phi)(4\cos\phi-3\cos\phi_1)-3a_2^2\{(A+q)(-2\phi\right.$$
$$\left.+\sin2\phi)+h_{D_1}\left(-2+\cos2\phi\right)\}+C_1^i\right] \quad (32)$$

The deformations follow by substituting Equations (2), (3), (30) and (32) for the middle-inner region of the toroidal vessel into Equations (8) and (9):

$$\left(\delta^m\right)_2^o = \frac{\gamma}{12Et\sin\phi}\left[\frac{A+q-a_2\sin\phi}{a_2\sin\phi}\{-a_2^3(-2+\cos2\phi)(4\cos\phi-3\cos\phi_1)\right.$$
$$-3a_2^2\{(A+q)(-2\phi+\sin2\phi)+h_{D_1}\left(-2+\cos2\phi\right)\}+C_1^i\}$$
$$-\nu\{a_2^3(3\cos\phi+\cos3\phi-3\cos\phi_1\cos2\phi)+3a_2^2((A+q)(2\phi-4\cos\phi_1\sin\phi$$
$$\left.+\sin2\phi)+h_{D_1}cos2\phi)+12a_2h_{D_1}(A+q)\sin\phi+C_1^i\}\right] \quad (33)$$

and

$$\left(V^m\right)_2^i = \frac{\gamma}{48Eta_2^2\sin^4\phi(A+q-a_2\sin\phi)}\left[-48a_2^5\sin^6\phi+6a_2^4(A+q)\sin\phi\{14-8\cos2\phi\right.$$
$$+2\cos4\phi+\cos\phi_1\left(-7\cos\phi+\cos^3\phi-3\cos\phi\sin^2\phi\right)\}+a_2^3(A+q)\{(A+q)(-81$$
$$+56\cos2\phi-7\cos4\phi+24\cos\phi_1\cos\phi+36\phi\sin2\phi)-3h_{D_1}\left(-8\sin2\phi+\sin4\phi\right)\}$$
$$-24a_2^2(A+q)^2\{2(A+q)(\phi\cos\phi-\sin\phi)+h_{D_1}\cos\phi\}-2(A+q)C_1^i\{4(A+q)$$
$$\left.\cos\phi-3a_2sin2\phi\}\right] \quad (34)$$

For the lower-inner region of the tank, substituting Equations (2), (3), and (4) into (6) and evaluating the integral, and using the condition that N_ϕ^m in the middle-inner region of the vessel and in the lower-inner region of the vessel must have the same values at the junction $\phi=\phi_2$ of the two regions, we obtain after some simplifications, the meridional stress resultant

$$\left(N_\phi^m\right)_3^i = \frac{\gamma}{12\sin\phi(A-a_3\sin\phi)}\{2a_3^3\cos^2\phi(2\cos\phi-3\cos\phi_2)+3a_3^2(A(2\phi-4\cos\phi_2\sin\phi$$

$$+\sin 2\phi) + 2h_{D_2}\cos^2\phi\big) + 12a_3 A h_{D_2}\sin\phi + C_2^i\Big\} \tag{35}$$

Where:

$$C_2^i = -a_3\Big\{-2a_3^2\cos^3\phi_2 + 12Ah_{D_2}\sin\phi_2 + a_3\big(-3A\sin 2\phi_2 + 6h_{D_2}\cos^2\phi_2 + 6A\phi_2\big)\Big\} + \frac{A - a_3\sin\phi_2}{A - a_1\sin\phi_2 + (a_2 - a_1)\sin\phi_1}\Big\{a_2^3\big(3\cos\phi_2 - 3\cos\phi_1\cos 2\phi_2 + \cos 3\phi_2\big) + 3a_2^2\big(h_{D_1}\cos 2\phi_2 + (A + (a_2 - a_1)\sin\phi_1)(-4\cos\phi_1\sin\phi_2 + \sin 2\phi_2 + 2\phi_2)\big) + 12a_2 h_{D_1}\sin\phi_2\big(A + (a_1 - a_2)\sin\phi_2\big) + C_1^i\Big\} \tag{36}$$

The hoop stress resultant follows as"

$$\big(N_\theta^m\big)_3^i = \frac{\gamma}{12a_3\sin^2\phi}\Big\{a_3^3\big(6\cos\phi - 2\cos 3\phi + 3\cos\phi_2(-3 + \cos 2\phi)\big) - 3a_3^2\big(A(-2\phi + \sin 2\phi) + h_{D_2}(-3 + cos2\phi)\big) + C_2^i\Big\} \tag{37}$$

Similarly, the deformations are:

$$\big(\delta^m\big)_3^i = \frac{\gamma}{12Et\sin\phi}\left[\left(\frac{A}{a_3\sin\phi} - 1\right)\Big\{a_3^3\big(6\cos\phi - 2\cos 3\phi + 3\cos\phi_2(-3 + \cos 2\phi)\big) - 3a_3^2\big(A(-2\phi + \sin 2\phi) + h_{D_2}(-3 + cos2\phi)\big) + C_2^i\Big\} - \nu\Big\{2a_3^3\cos^2\phi\big(2\cos\phi - 3\cos\phi_2\big) + 3a_3^2\big(A(2\phi - 4\cos\phi_2\sin\phi + \sin 2\phi) + 2h_{D_2}\cos^2\phi\big) + 12a_3 A h_{D_2}\sin\phi + C_2^i\Big\}\right] \tag{38}$$

and

$$\big(V^m\big)_3^i = \frac{\gamma}{48Eta_3^2\sin^4\phi\big(-A + a_3\sin\phi\big)}\Big[48a_3^5\sin^6\phi + 6a_3^4 A\sin\phi\Big\{-14 + 8\cos 2\phi - 2\cos 4\phi + \cos\phi_2\big(13\cos\phi - \cos^3\phi + 3\cos\phi\sin^2\phi\big)\Big\} + a_3^3 A\Big\{A\big(81 - 56\cos 2\phi + 7\cos 4\phi - 48\cos\phi_2\cos\phi - 36\phi\sin 2\phi\big) + 3h_{D_2}\big(-14\sin 2\phi + \sin 4\phi\big)\Big\} + 48a_3^2 A^2\Big\{A\big(\phi\cos\phi - \sin\phi\big) + h_{D_2}\cos\phi\Big\} + 2AC_2^i\big\{4A\cos\phi - 3a_3 sin2\phi\big\}\Big] \tag{39}$$

5. ACTUAL MEMBRANE STRESSES

In the usual way, the actual membrane stresses at a given point in question in the segmented toroidal shell are obtained by simply dividing the membrane stress-resultant values by the thickness of the shell at that point:

$$\sigma_\phi^m = \frac{N_\phi^m}{t} \tag{40}$$

$$\sigma_\theta^m = \frac{N_\theta^m}{t} \tag{41}$$

where σ_ϕ^m and σ_θ^m are the stresses in the meridional and hoop directions, respectively. With these final expressions, the formulated results for the membrane stress resultants are also valid for non-uniform shell-thickness variations.

6. NUMERICAL EXAMPLE

A toroidal shell of segmented spherical cross-section with a geometrical configuration that is not symmetrical about the equatorial plane is analysed. This example is particularly considered to show that the formulated results can also be applied to segmented toroids that are not symmetrical about the equatorial (middle) plane. The numerical values for the geometric, material and loading parameters of the toroid are

Outer region: $\phi_1 = 80^o;\ \phi_2 = 120^o;$

Inner region: $\phi_1 = 100^o;\ \phi_2 = 60^o;$

$A = 23.57\ mm;\ a_1 = 14.31\ mm;\ a_2 = 14.31\ mm;\ a_3 = 14.31\ mm;\ t = 0.05\ mm;\ E = 200\ GPa;$ $\nu = 0.3;$ and $\gamma = 10\times10^3\ N/m^3$. To obtain the membrane results for most of the middle surfaces of the vessel without the interference of support effects, a hypothetical location of the support at the region of the lower circle of latitude, far enough, at least 30^o from the lower edge location of the vessel is assumed. As it is well-known (Zingoni, 1997; Blaauwendraad and Hoefakker, 2014; Zingoni et al., 2015), the best location of the support will be at the equatorial plane (the innermost and outermost circles of latitude), where the support reaction will be tangential to the shell middle surface, hence providing less bending disturbances at that region. A numerical modelling will be required to determine the behaviour of the shell in the support region of the vessel which, as earlier mention, is beyond the scope of the present study. The variations of stresses with angular coordinate ϕ over the full profile of the vessel are shown in Figures (3) and (4). Note that the values below $\phi = 20^o$ and beyond $\phi = 160^o$ at the outer and inner regions of the vessel are not presented in the Figures, since membrane solution cannot be used to estimate the state of stress in the vicinity of the top and bottom circles of latitude without additional bending due to the incompatibility of deformations at the meeting points of the synclastic and anticlastic surfaces of the toroidal shell (Novozhilov, 1951; Bickell and Ruiz, 1967; Flügge, 1973; Ventsel and Krauthammer, 2001).

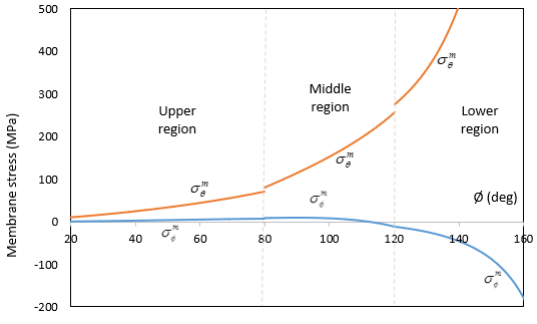

Figure 3: Variations of membrane stresses over the outer cross-sectional profile of the toroidal vessel

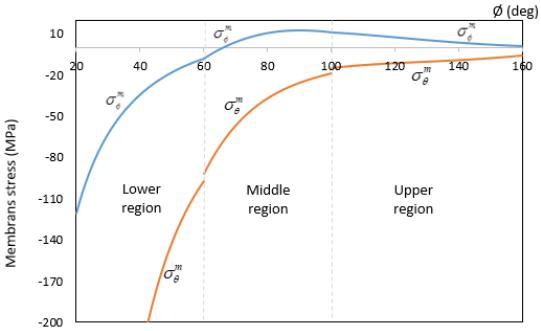

Figure 4: Variations of membrane stresses over the inner cross-sectional profile of the toroidal vessel

7. DISCUSSION OF RESULTS

In the upper-outer region of the vessel, Figure 3, σ_ϕ^m gradually rise in tension as one moves from the apex towards the upper-outer edge $\phi = 80^o$ attaining a value of 7.66 MPa, while σ_θ^m appreciably rise in tension to a value of 66.98 MPa. The corresponding membrane deformations δ^m and V^m are 12.75 mm and -1.25×10^3 respectively. At the junction $\phi = 80^o$, there are discontinuities in σ_θ^m, δ^m and V^m, but not in σ_ϕ^m in moving across the junction to the middle-outer region, where σ_θ^m, δ^m and V^m become 79.60 MPa, 14.56 mm and -1.39×10^3 respectively at the upper-outer edge of the middle-outer region of the vessel.

In the middle-outer region, the meridional stress σ_ϕ^m continues to rise until it reaches a maximum tensile value of 8.55 MPa at $\phi = 90^o$ (around the equator), then began to decrease beyond that point to zero at approximately $\phi = 111.5^o$, becoming compressive afterwards to attain a compressive value of -11.55 MPa at the lower-outer edge $\phi = 120^o$. The hoop stress σ_θ^m continues to rise more appreciably from the upper-outer edge to the lower-outer edge, where it attained a value of 255.85 MPa. The corresponding membrane deformations δ^m and V^m are 44.68 mm and -2.09×10^3 respectively. Just as in the upper- outer edge, at the junction $\phi = 120^o$, there are discontinuities in σ_θ^m, δ^m and V^m, but not in σ_ϕ^m in moving across the junction to the lower-outer region, where σ_θ, δ^m and V^m become 275.40 MPa, 4.00 mm and -4.89×10^3 respectively at the lower-outer edge of the lower-outer region of the vessel. Both σ_ϕ^m and σ_θ^m thereafter in the lower-outer region of the vessel continue to increase more and rapidly in compression and tension, respectively, with ϕ. In the outer regions of the vessel, it is noted that the hoop stress σ_θ^m is tensile throughout the vessel with relatively large values at the lower parts. The meridional stress σ_ϕ^m became compressive in the lower parts of the vessel (from $\phi = 111.5^o$) indicating that stiffeners should be added to, or the thickness of the shell *t* should be increased in these regions to avoid buckling of the vessel, which will be more prevalent in much larger vessels. The values of the horizontal displacement δ^m obtained at the edges of the outer region of the vessel, though generally small, show that all edges move laterally outwards of the axis of revolution of the toroid as expected of the internally contained water.

In the lower-outer region of the vessel (Figure 4), both σ_ϕ^m and σ_θ^m significantly decrease in magnitude as one moves from the base towards the lower-inner edge $\phi = 60^o$ to -8.16 MPa and -97.42 MPa (compressive) respectively. The corresponding membrane deformations δ^m and V^m are -6.02 mm and 1.35×10^3 respectively. At the junction $\phi = 60^o$, there are discontinuities in σ_θ^m, δ^m and V^m, but not in σ_ϕ^m in moving across the junction to the middle-inner region, where σ_θ^m, δ^m and V^m become -92.35 MPa, -5.70 mm and 0.97×10^3 respectively at the lower-inner edge of the middle-inner region of the vessel.

In the middle-inner region, the meridional stress σ_ϕ^m continues to decrease in magnitude until it reaches zero at approximately $\phi = 66^o$, then began to increase in tension beyond that point to a maximum tensile

value of 12.63 MPa at $\phi = 90^o$ (around the inner equator). It then began to decrease from the maximum tensile value to attain a value of 11.15 MPa at the upper-inner edge $\phi = 100^o$. The hoop stress σ_θ^m continues to reduce less appreciably from the lower-inner edge to the upper-inner edge, where it reaches a value of -18.78 MPa. The corresponding membrane deformations δ^m and V^m are -1.05 mm and 3.29×10^5 respectively. Just as in the lower-inner edge, at the junction $\phi = 100^o$, there are discontinuities in σ_θ^m, δ^m and V^m, but not in σ_ϕ^m in moving across the junction to the upper-inner region, where σ_θ, δ^m and V^m become -15.24 MPa, -0.88 mm and 2.98×10^5 respectively at the upper-inner edge of the upper-inner region of the vessel. Both σ_ϕ^m and σ_θ^m thereafter in the upper-inner region of the vessel continue to decrease but more gradually in tension and compression respectively with ϕ.

The meridional stress σ_ϕ^m is only compressive in the lower parts of the vessel, while the hoop stress σ_θ^m is compressive throughout the inner region of the vessel with relatively large hoop compression at the lower parts, indicating that stiffeners should be added to, or the thickness of the shell t should be increased in these regions to avoid local buckling of the vessel. The values of the horizontal displacement δ^m obtained at the edges of the inner region of the vessel show that all edges move laterally inwards of the axis of revolution of the toroid as expected of the internally contained water.

The maximum tensile value of meridional stress at the inner regions of the vessel is higher than that at the outer regions of the vessel, indicating that the vessel will most likely fail in the inner region. These maximum tensile values occur at the equator $(\phi = 90^o)$ of the vessel for both the outer and inner regions. It will suffice to note here that bending will occur around the edges of the vessel, due to the discontinuities in the deformations there.

8. CONCLUSION

Based on the theory of shells of revolution, explicit expressions have been formulated for determining the membrane stresses and deformations that occur within an assembly of toroidal shell segments for liquid containment. The cross-section of the vessel is physically similar to that of an elliptical toroid. In comparison with an elliptical toroid, the vessel can be fabricated easily due to the constant radius of curvature within a particular segment of the vessel. A numerical example has been presented for a toroid of segmented spherical cross-section with geometrical configuration that is not symmetrical about the equatorial plane. The vessel was assumed to be completely-filled with water of approximate specific weight $\gamma = 10\times10^3\ N/m^3$. A set of design recommendation has been provided. Local buckling may likely occur around the segments in the lower regions of the vessel due to the compressive stresses experienced there. It is observed that there are discontinuities in the hoop stresses and deformations at the junctions of the vessel. These may be accounted for by employing the general bending theory of shells of revolution. The presented analytical results can also be used for conducting parametric studies, and as pre-buckling results for buckling analysis of the vessel.

9. ACKNOWLEDGEMENT

The first author greatly appreciates the assistance provided through the Bathe SEMC PhD Scholarship and JW Jagger Centenary Gift Scholarship.

10. CONFLICT OF INTEREST

There is no conflict of interest associated with this work.

REFERENCES

Bickell, M. B. and Ruiz, C. (1967). *Pressure vessel design and analysis*. London: Macmillan and Company Limited.

Blaauwendraad, J. and Hoefakker, J. H. (2014). *Structural Shell Analysis*. London: Springer.

Burgos, C. A. Jaca, R. C., Lassig, J. L. and Godoy, L. A. (2014). Wind buckling of tanks with conical roof considering shielding by another tank. *Thin-Walled Structures*, 84, pp. 226–240.

Enoma, N. and Zingoni, A. (2017). Analytical formulation and numerical modelling for multi-shell toroidal pressure vessels. *Computers and Structures*. (In press)

Flügge, W. (1973). *Stresses in shells*. Berlin: Springer-Verlag.

Guggenberger, W. (1994). Collapse design of large steel digester tanks. *Thin-Walled Structures*, 20(1–4), pp. 109–128.

Kuznetsov, V. V. and Levyakov, S. V. (2001). Nonlinear pure bending of toroidal shells of arbitrary cross-section. *International journal of solids and structures*, *38*(40-41), pp. 7343-7354.

Novozhilov, V. V (1951). *The theory of thin shells*. The Netherlands: Wolters-Noordhoff Publishing.

Ozdemir, Z., Souli, M. and Fahjan, Y. M. (2010). Application of nonlinear fluid–structure interaction methods to seismic analysis of anchored and unanchored tanks. *Engineering Structures*, 32(2), pp. 409–423.

Redekop, D., Xu, B. and Zhang, Y. M. (1999). Stability of a toroidal fluid-containing shell. *International Journal of Pressure Vessels and Piping*, 76, pp. 575–581.

Rotter, J. M. (1998). Shell structures: The new European standard and current research needs. *Thin-Walled Structures*, 31(1–3), pp. 3–23.

Sosa, E. M. and Godoy, L. A. (2010). Challenges in the computation of lower-bound buckling loads for tanks under wind pressures. *Thin-Walled Structures*, 48(12), pp. 935–945.

Sosa, E. M., Godoy, L. a. and Croll, J. G. (2006). Computation of lower-bound elastic buckling loads using general-purpose finite element codes. *Computers and Structures*, 84(29–30), pp. 1934–1945.

Taniguchi, T., Ando, Y. and Nakashima, T. (2009). Fluid pressure on unanchored rigid flat-bottom cylindrical tanks due to uplift motion and its approximation. *Engineering Structures*, 31(11), pp. 2598–2606.

Teng, B. G., Yuan, S. J. and Wang, Z. R. (2002). Effect of the initial structure on the hydro-forming of toroidal shells. *Journal of Materials Processing Technology*, 123, pp. 18–21.

Velickovic, V. (2007). Stress and strain states in the material of the stressed toroidal container for liquefied petroleum gas. *Scientific Technical Review*, 57(3), pp. 94–105.

Ventsel, E. and Krauthammer, T. (2001). *Thin plates and shells: theory, analysis, and applications*. New York: Marcel Dekker, Inc.

Zhan, H. J. and Redekop, D. (2008). Vibration, buckling and collapse of ovaloid toroidal tanks. *Thin-Walled Structures*, 46(4), pp. 380–389.

Zhang, Y. M., Mirfakhraei, P., Xu, B. and Redekop, D. (1998). A computer program for the elastostatics of a toroidal shell using the differential quadrature method. *International Journal of Pressure Vessels and Piping*, 75, pp. 919–929.

Zingoni, A. (1997). *Shell structures in civil and mechanical engineering*. London: Thomas Telford Publishing.

Zingoni, A. (2001a). Stresses and deformations in egg-shaped sludge digestors: discontinuity effects. *Engineering Structures*, 23(11), pp. 1373–1382.

Zingoni, A. (2001b). Stresses and deformations in egg-shaped sludge digestors: membrane effects. *Engineering Structures*, 23, pp. 1365–1372.

Zingoni, A. (2002). Parametric stress distribution in shell-of-revolution sludge digesters of parabolic ogival form. *Thin-Walled Structures*, 40, pp. 691–702.

Zingoni, A. (2004). On analytical solutions for liquid-filled non-shallow conical shell assemblies. *Journal of the South African Institution of Civil Engineering*, 46(3), pp. 10–15.

Enoma, N. and Zingoni, A. (2016). Stresses in multi-shell toroidal pressure vessels. In Zingoni, A. (ed.) (2016). *Insights and Innovations in Structural Engineering, Mechanics and Computation. Proceedings of the Sixth International Conference on Structural Engineering, Mechanics and Computation (SEMC 2016), 5-7 September 2016, Cape Town, South Africa.* London: Taylor & Francis Group, pp. 799–805.

Zingoni, A., Mokhothu, B. and Enoma, N. (2015). A theoretical formulation for the stress analysis of multi-segmented spherical shells for high-volume liquid containment. *Engineering Structures*. Elsevier Ltd, 87, pp. 21–31.

Zu, L., Zu, L., Zhang, D., Xu, Y. and Xiao, D. (2012a). Integral design and simulation of composite toroidal hydrogen storage tanks. *International Journal of Hydrogen Energy*, 37, pp. 1027–1036.

Zu, L., Koussios, S. and Beukers, A. (2012b). A novel design solution for improving the performance of composite toroidal hydrogen storage tanks. *International Journal of Hydrogen Energy*, 37, pp. 14343–14350.